RESEARCH ARTICLE

Open Access



Decidual stromal cells-derived exosomes incured insufficient migration and invasion of trophoblast because of abnormal ubiquitination and degradation of Snail mediated by miR-92b-3p/USP28

Miao Xiong^{1,2†}, Ziqiu He^{1†}, Liping Wen¹ and Aimin Zhao^{2*}

Abstract

Background Recent findings have demonstrated that inadequate trophoblast migration and invasion are often responsible for the unsuccessful communication between the mother and fetus, contributing to URSA (unexplained recurrent spontaneous abortion). Effective intercellular communication at the maternal–fetal interface is crucial for maintaining trophoblast invasion and migration. Decidual stromal cells (DSCs), which are predominant at the maternal–fetal interface, have been identified as key regulators of the epithelial-mesenchymal transition (EMT) of trophoblasts, which facilitates their migration and invasion. However, the underlying biological mechanisms remain largely unexplored and constitute the central focus of this study.

Results The inhibition of trophoblast EMT by URSA-DSC-derived exosomes (URSA-DSC-exos) resulted in decreased migration and invasion abilities in vitro. MicroRNA sequencing revealed that miR-92b-3p were the most significantly upregulated microRNA in trophoblasts treated with URSA-DSC-exos. Further functional experiments demonstrated that URSA-DSC-exos inhibited trophoblast migration and invasion by transferring miR-92b-3p. Mechanistically, miR-92b-3p in URSA-DSC-exos suppressed trophoblast migration and invasion by directly downregulating USP28 expression at the post-transcriptional level. Overexpression of USP28 rescue the inhibitory effect of miR-92b-3p mimics on the expression of USP28 and restored the invasion and migration capabilities of HTR-8/SVneo cells. Furthermore, in vivo experiment suggested that URSA-DSC-exos led to increased embryo absorption in mice. Clinically, alterations in USP28 and EMT-related molecule expressions were observed in URSA patients, and a negative correlation was noted between miR-92b-3p and USP28 levels.

Conclusion Our findings has demonstrated that the induction of insufficient migration and invasion of trophoblast by URSA-DSC-exos is due to abnormal ubiquitination degradation, which is mediated by the low expression of USP28, which is suppressed by miR-92b-3p at the post-transcriptional level. Reversing this disorder sheds light on a novel mechanism in DSC regulation of trophoblasts, highlighting their significant role in URSA.

[†]Miao Xiong and Ziqiu He contributed equally to this work.

*Correspondence:
Aimin Zhao
zamzkh0526126.com@sjtu.edu.cn
Full list of author information is available at the end of the article



© The Author(s) 2025. **Open Access** This article is licensed under a Creative Commons Attribution-NonCommercial-NoDerivatives 4.0 International License, which permits any non-commercial use, sharing, distribution and reproduction in any medium or format, as long as you give appropriate credit to the original author(s) and the source, provide a link to the Creative Commons licence, and indicate if you modified the licensed material. You do not have permission under this licence to share adapted material derived from this article or parts of it. The images or other third party material in this article are included in the article's Creative Commons licence, unless indicated otherwise in a credit line to the material. If material is not included in the article's Creative Commons licence and your intended use is not permitted by statutory regulation or exceeds the permitted use, you will need to obtain permission directly from the copyright holder. To view a copy of this licence, visit https://creativecommons.org/licenses/by-nc-nd/4.0/.

Xiong et al. BMC Biology (2025) 23:222 Page 2 of 20

Keywords Decidual stromal cells, Exosomes, Epithelial-mesenchymal transition, Ubiquitination degradation, Ubiquitin-specific protease 28

Background

The successful initiation and maintenance of a healthy pregnancy rely on the efficient exchange of biological information between the mother and embryo [1]. This process involves the timely penetration and invasion of trophoblasts into the endometrium and superficial myometrium, coupled with the remodeling of uterine spiral arteries [2-4]. Concurrently, endometrial decidualization takes place, ensuring optimal endometrial receptivity and preparation for embryo implantation [5, 6]. Trophoblasts, which are pivotal in the remodeling of uterine spiral arteries, have the capability to proliferate, differentiate, migrate, and invade [7, 8]. Decidualization refers to the transformation of endometrial stromal cells (ESCs) into specialized secretory DSCs [9, 10], creating an environment conducive to immune regulation and nutrition, thereby facilitating embryo implantation and normal placental development [11, 12]. If communication between trophoblasts and DSCs at the maternal-fetal interface is disrupted, it may result in impaired trophoblast migration and invasion [13], leading to pathological changes such as shallow placental implantation and compromised microvascular formation [14]. These conditions may contribute to a spectrum of pregnancy complications, including recurrent spontaneous abortion (RSA), fetal growth restriction (FGR), preeclampsia (PE), and premature birth [15–21]. RSA, characterized by two or more consecutive spontaneous abortions, affects 5% of pregnancies [22, 23]. While various factors have been identified as contributors to RSA, including chromosomal abnormalities, reproductive tract infections, anatomical abnormalities, endocrine disorders, autoimmune abnormalities, and thrombophilia, etc. [24], however, nearly 50% of RSA patients have no identifiable cause, classified as URSA [25, 26]. Due to the elusive etiology and pathogenesis of URSA, there is a lack of clinically recognized and effective treatment methods. Consequently, deepening our understanding of the pathogenesis of URSA, identifying potential treatment targets, and establishing appropriate treatment methods hold significant theoretical and practical implications. Recent studies have highlighted the importance of trophoblast development in ensuring successful embryo implantation and pregnancy [27-30]. Impaired trophoblast invasion and migration have been associated with uteroplacental insufficiency, thereby increasing the risk of RSA, FGR, and PE [31]. However, the underlying biological mechanisms remain largely unknown and are the focus of ongoing research. Gaining a more comprehensive understanding of the molecular pathways underpinning placental EMT and the signaling pathways governing developmental program could unveil novel therapeutic strategies aimed at improving feto-placental growth in pregnancy complications such as PE, RSA, and FGR.

In recent years, the role of microRNAs in regulating downstream target genes at the post-transcriptional level has gained considerable interest [32]. MicroR-NAs (miRNAs) are small, siRNA-like molecules found in eukaryotes, acting as endogenous non-coding RNAs with regulatory functions [33]. These molecules, ranging between 18 and 25 nucleotides in length, are generated from longer primary transcripts through a series of nuclease-mediated processing events [33]. Mature miRNAs subsequently assemble into the RNA-induced silencing complex (RISC), which identifies target mRNA through base-pair complementarity. Consequently, RISC can mediate the degradation of target gene mRNA or impede target gene translation by binding to the 3'UTR or ORF region of the target gene mRNA [34, 35]. Extensive research has revealed that miRNAs can stably exist in various bodily fluids, such as saliva, urine, amniotic fluid, breast milk, and blood. Furthermore, studies have shown that miRNAs can be loaded into extracellular vesicles, which act as carriers for information transmission between cells. This mode of communication is considered the third form of cellular information exchange. Substantial evidence supports the notion that miRNAs transferred through exosomes can regulate maternal-fetal homeostasis [36–38]. Investigating the effects of miRNAs on trophoblast biology and their underlying mechanisms may contribute to a deeper understanding of the pathophysiological processes associated with RSA.

Considering the interactions between DSC and trophoblasts at the maternal-fetal interface [6, 10, 13], along with the crucial role of exosomes in facilitating intercellular communication, we hypothesized that URSA-associated DSC may inhibit the EMT of trophoblasts. The differentiation of human cytotrophoblast cells (CTB) into extravillous trophoblast cells (EVT) is characterized as an EMT process [39, 40]. Polarized CTB, situated within an epithelial layer, undergo transformation into motile, non-polar EVTs that invade the uterus [41]. Extravillous trophoblasts play a key role in penetrating the maternal decidua and

Xiong et al. BMC Biology (2025) 23:222 Page 3 of 20

thereby establishing a connection with the maternal spiral arteries. Dysregulation of this process can lead to adverse pregnancy outcomes, such as RSA and PE [6, 21]. Therefore, the meticulous regulation of this EMT is crucial for a successful pregnancy.

This inhibition is achieved through the secretion of extracellular vesicles, which impair the invasive and migratory capacity of trophoblasts, leading to the development of URSA. To explore this hypothesis, the present study utilized a combination of in vitro, in vivo, and clinical samples, aiming to provid insights into the novel mechanisms that regulate trophoblast function and lead to the pathogenesis of URSA, thereby offering potential therapeutic targets. The details are as follows.

Results

PKH67-labeled DSC-exos or ESC-exos binding with the trophoblasts

Enzyme digestion and adherent methods have proven effective in eliminating fibroblast contamination in primary isolated DSCs and ESCs. ESCs, sourced from the secretory endometrium, and DSCs, derived from earlypregnancy decidua, exhibit an irregular polygonal shape. DSCs possess a more abundant cytoplasm and larger cell size compared to ESCs, as observed under an optical microscope, aligning with findings reported in existing literature [42, 43]. Immunofluorescence staining further confirmed these isolated cells as stromal cells, evidenced by their expression of Vimentin (indicative of mesenchymal origin, green fluorescence) and the absence of cytokeratin 7 expression (specific to epithelial cells, red fluorescence) (Fig. 1A). Recent studies have demonstrated that DSCs secrete and transfer exosomes, rich in signaling molecules, to adjacent cells. Based on this, we hypothesized that extracellular vesicles derived from DSCs could negatively impact the migration and invasion capabilities of trophoblasts in vitro. We isolated exosomes from the supernatant of DSCs, utilizing decidual specimens of URSA patients and normal pregnancies, with ESCs serving as a comparative control. TEM analysis depicted the presence of double concave discshaped bilayer membrane structures in N-DSC-Exos, URSA-DSC-exos, and N-ESC-exos, exhibiting a saucerlike appearance (Fig. 1B). WB further validated that specific markers CD81, CD63, CD9,TSG101, and HSP70 were abundantly present in DSC-exos and ESC-exos, Simultaneously Calnexin (negative control) were not present in DSC-exos or ESC-exos, confirming successful exosome isolation (Fig. 1C and Additional file 1). NTA revealed that these rounded particles had a size distribution of 30-200 nm, and there was a certain difference in the number and concentration of DSC-exos between the URSA patients and the normal pregnancy women, which may also be one of the reasons for the functional differences between these two types of DSC-exos. (Fig. 1D). The above methodology strictly follow the recommendations for extracelluar vesicles (EV) studies described in the MISEV2018 guidelines [44] to ensure the reliability and reproducibility of EV research.

Subsequent investigations focused on whether DSC-exos or ESC-exos binding with HTR-8/SVneo cells. After purifying and labeling DSC-exos or ESC-exos with PKH67, the labeled exosomes were incubated with HTR-8/SVneo cells for 12, 24, and 48 h. Laser confocal microscopy illustrated that after 12 h, PKH67-labeled DSC-exos or ESC-exos binding with the HTR-8/SVneo cells (Fig. 1E).

URSA-DSC-exos suppress EMT, migration, and invasion of trophoblast in vitro

As showed in our previous study [43], trophoblasts cocultured with URSA-DSC-exos exhibited a decrease in wound closure and a diminished invasive potential compared to those cultured with N-ESC-exos. The results of WB and qRT-PCR revealed an upregulation of the epithelial marker E-cadherin and a downregulation of the mesenchymal marker N-cadherin in HTR-8/SVneo cells after co-culture with URSA-DSC-exos. However, notably decreased protein levels was observed in Snail expression in trophoblast HTR-8/SVneo treated with URSA-DSCexos, while Vimentin expression remained unaffected by URSA-DSC-exos.

Synergistic effect of URSA-DSC-exos derived mR-92b-3p and miR-22-5p_R-1 on the trophoblast invasion and migration

To elucidate the potential mechanisms by which DSCexos influence trophoblast migration and invasion, we performed miRNA sequencing on exosomes obtained from both normal and URSA patient's DSCs. It was found that, compared with the N-DSC-exos, the URSA-DSC-exos showed significantly higher expression of miR-92b-3p and miR-22-5p_R-1. Furthermore, our previously analysis revealed that URSA-DSC-exos can transport miR-92b-3p and miR-22-5p R-1 into trophoblasts [43]. In the subsequent target gene prediction and validation process, we found that miR-22-5p_R-1 and its target gene, PDK4 (pyruvate dehydrogenase kinase 4), appear to be involved in the invasion and migration of trophoblasts by regulating the energy metabolism phenotype of trophoblast [43]. Interestingly, co-transfection of miR-92b-3p and miR-22-5p-R-1 mimics revealed a stronger effect than either single transfection. Transwell and wound healing showed that when HTR-B/SVneo were co-transfected with miR-92b-3p and miR-22-5p-R-1 mimics, their invasion and migration abilities decreased

Xiong et al. BMC Biology (2025) 23:222 Page 4 of 20

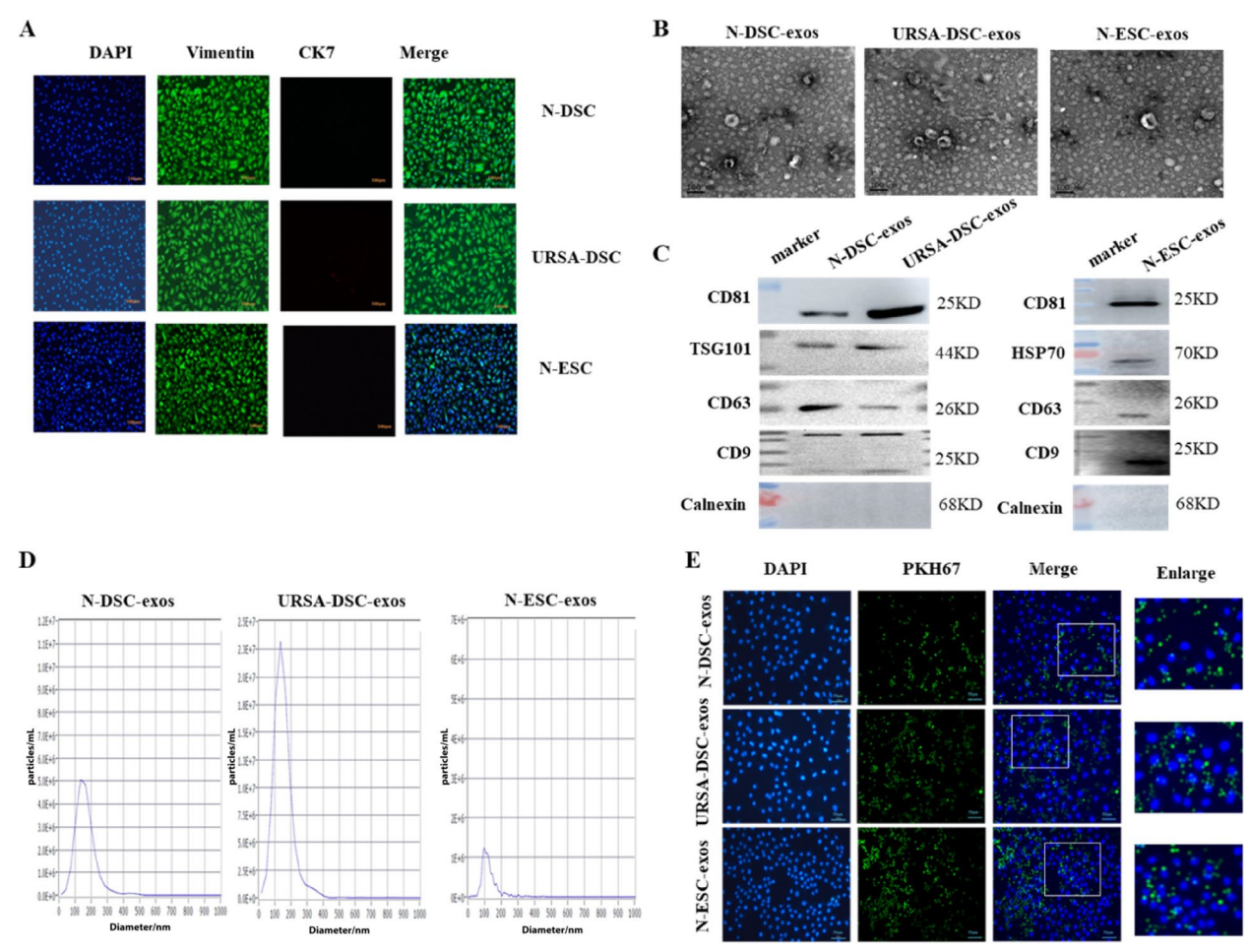


Fig. 1 PKH67-labeled DSC-exos or ESC-exos blinding with the trophoblasts (n = 36, means ± SD). **A** Immunofluorescence was utilized to identify both DSCs and ESCs. The mesenchyme origin-specific Vimentin (green) and the epithelial cells-specific CK7 (red) were employed to identify DSCs and ESCs (scale bar, 100 μm). **B** Exosome examination was conducted through TEM, as detailed in the supplementary information methods. **C** WB analysis revealed the expression of secretory marker proteins TSG101, CD81, CD9, CD63, and no expression of Calnexin (negative control) in exosomes derived from N-DSC and URSA-DSC. The N-ESC-Exos displayed expression of characteristic exosomal markers, including CD81, HSP70, CD9, and CD63, with no expression of Calnexin. **D** NTA was employed to verify particle sizes and concentrations, confirming the presence of exosomes. **E** Laser confocal fluorescence microscopy images depicted HTR8/SVneo cell incubation with PKH67-labeled N-DSC-exos, URSA-DSC-exos, or N-ESC-exos (in green) at time points of 12 h (scale bar, 50 μm). Full-length blots/gels are presented in Additional file 1[Aikira1] [Aikira1] [Aikira1] [Existinal] Existinal (Paikira1) [Aikira1] [Aikira1]

more significantly than when miR-92b-3p or miR-22-5p-R-1 mimics transfected alone (p < 0.05) (Fig. 2A,B).

MiR-92b-3p suppresses EMT, migration, and invasion of trophoblasts

To assess the impact of miR-92b-3p on trophoblast migration and invasion, we introduced miR-92b-3p mimics or miR-92b-3p inhibitors into HTR-8/SVneo cells. Our findings revealed that miR-92b-3p mimics significantly reduced Snail protein expression while increasing E-cadherin expression, without influencing Vimentin and N-cadherin expression. Conversely, the miR-92b-3p inhibitors exhibited the opposite effects in HTR-8/

SVneo cells (Fig. 3A,B and Additional file 1). Additionally, wound healing and transwell assays showed that miR-92b-3p mimics slowed wound closure in HTR-8/SVneo cells and diminished cell invasion compared to the control group, whereas inhibitors demonstrated opposite outcomes (Fig. 3C,D).

USP28 is the common target of miR-92b-3p

Numerous studies have demonstrated that miRNAs primarily exert their biological functions by regulating the expression of downstream target genes. To analyze the target genes of miR-92b-3p, KEGG and GO enrichment analyses were performed using the Miranda and

Xiong et al. BMC Biology (2025) 23:222 Page 5 of 20

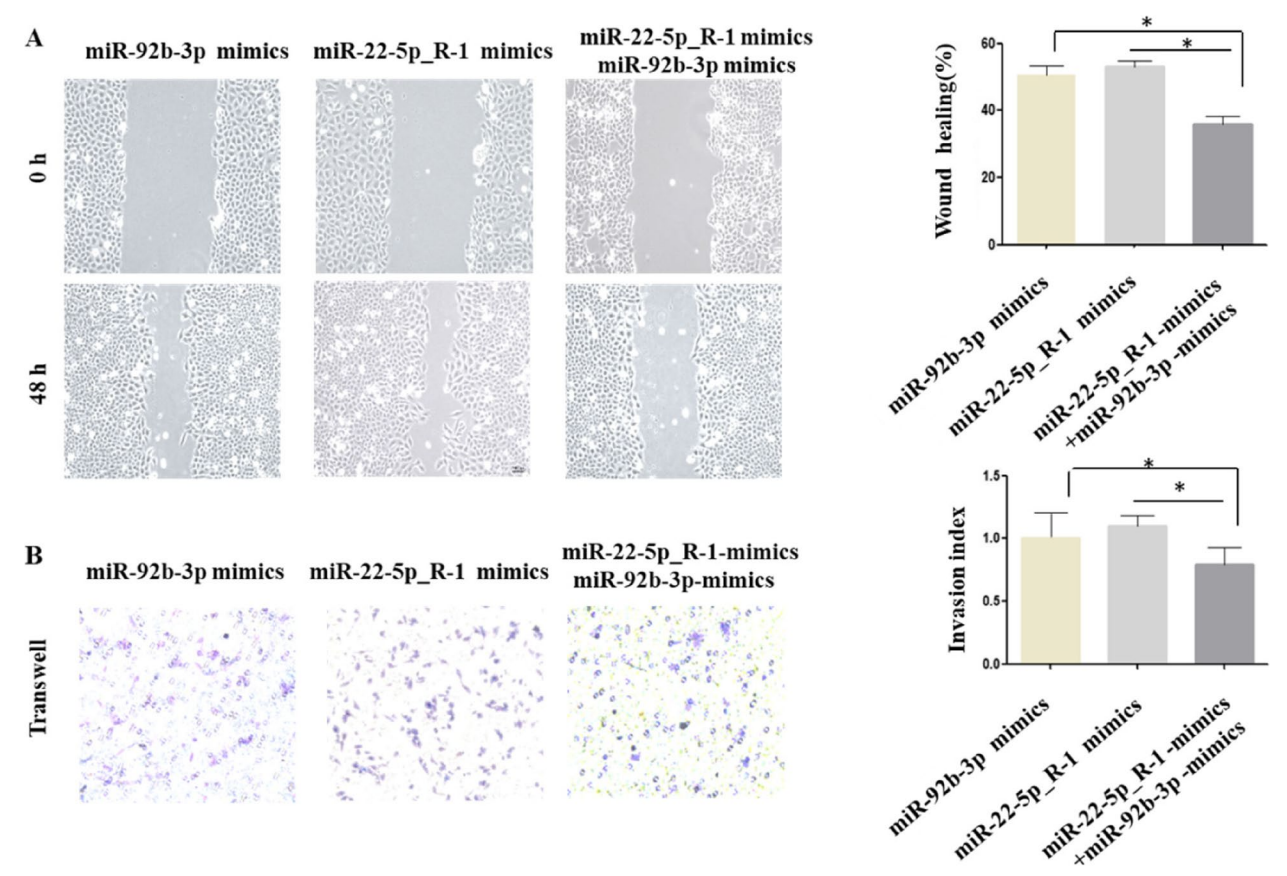


Fig. 2 Synergistic effect of miR-92b-3p and miR-22-5p_R-1 on the trophoblast invasion and migration. **A** Evaluating of the migration capacity of HTR-8/SVneo cells 48 h after transfection with miR-92b-3p mimics alone or co-transfection with miR-92b-3p mimics and miR-22-5p_R-1 mimics using wound healing. **B** Investigation of the invasion capacity of HTR-8/SVneo cells 48 h post-transfection with miR-92b-3p mimics alone or co-transfection with miR-92b-3p mimics and miR-22-5p_R-1 mimics via transwell assays. Representative images of migrated or invaded cells are provided (magnification, × 20). All experiments were repeated 6 times to ensure the accuracy of the data. The results are expressed as average ± standard deviation (SD). Data were analyzed by one-way ANOVA with Tukey's post hoc test. Error bars indicate standard deviation. SD. **p < 0.01

Targetscan databases. The results of the KEGG enrichment analysis were represented in a bubble chart using ggplot2, where RichFactor denotes the ratio of target genes to the total number of genes in the KEGG pathway. A higher RichFactor value indicates greater KEGG enrichment (Fig. 4A). The first 20 KEGG pathways with the lowest p-values were plotted, with the x-axis representing the p-log10 value of the enriched KEGG pathway analysis and the y-axis indicating the pathway name (Fig. 4B). Both the KEGG bubble and bar plots showed enrichment in the ubiquitin-proteasome system, corroborating the experimental results obtained. Subsequently, the Miranda and Targetscan public databases were utilized to predict the target genes of miR-92b-3p (Fig. 4C), identifying four common target genes for miR-92b-3p (Fig. 4D). An miRNA online database prediction revealed potential binding sites for miR-92b-3p targets within the USP28 3'-UTR (Fig. 4E). To verify whether USP28 is a direct target of miR-92b-3p, mutant or wild-type miRNA binding site USP28 3'-UTR-driven luciferase vectors were cotransfected into HTR-8/SVneo cells with miR-92b-3p mimics or inhibitors. The dual-luciferase reporter assay results demonstrated significant reduction in luciferase activity in the WT-USP28-3'UTR+miR-92b-3p mimics group, with this inhibition rescued by miR-92b-3p mimics binding site mutations (Fig. 4F). To further assess the effects of miR-92b-3p on USP28 expression, miR-92b-3p mimics and their inhibitors were transfected into HTR-8/SVneo cells. The findings revealed that miR-92b-3p mimics decreased USP28 expression, whereas their inhibitors produced opposite effects in HTR-8/SVneo cells (Fig. 4G and Additional file 1). Overall, our data suggest that USP28 was a common target of miR-92b-3p.

Xiong et al. BMC Biology (2025) 23:222 Page 6 of 20

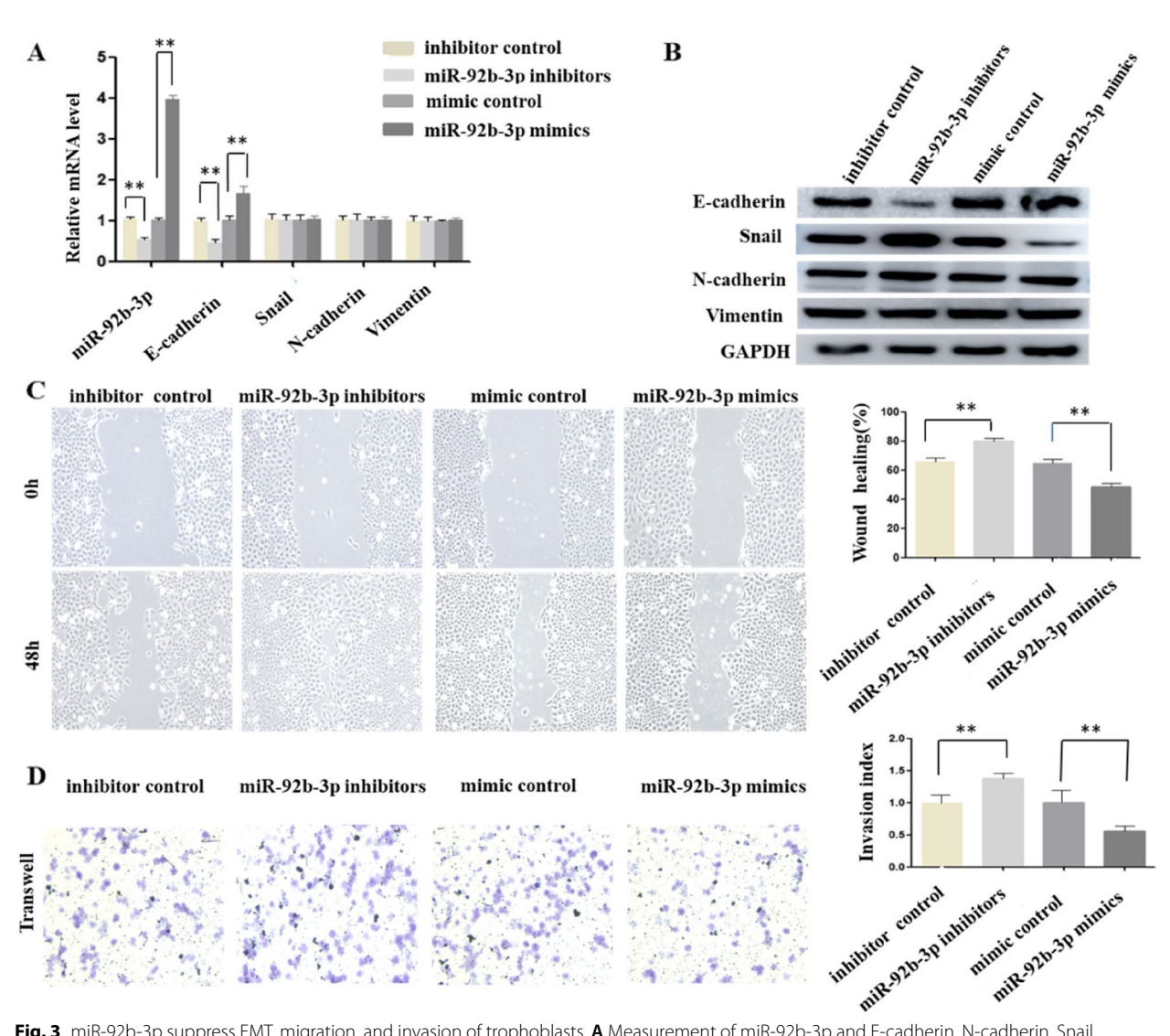


Fig. 3 miR-92b-3p suppress EMT, migration, and invasion of trophoblasts. A Measurement of miR-92b-3p and E-cadherin, N-cadherin, Snail, and Vimentin mRNA expression levels in HTR-8/SVneo cells using qRT-PCR 48 h following transfection with miR-92b-3p mimics or inhibitors. B Assessment of E-cadherin, N-cadherin, Snail, and Vimentin protein levels using WB analysis 48 h following transfection with miR-92b-3p mimics or inhibitors. C Evaluating of the migration capacity of HTR-8/SVneo cells 48 h after transfection with miR-92b-3p mimics or inhibitors using wound healing assays. D Investigation of invasion capacity of HTR-8/SVneo cells 48 h post-transfection with miR-92b-3p mimics or inhibitors via transwell assays. Representative images of migrated or invaded cells are provided (magnification, \times 20). All experiments were repeated 6 times to ensure the accuracy of the data. The results are expressed as the average \pm standard deviation (SD). Data were analyzed by one-way ANOVA with Tukey's post hoc test. Error bars indicate standard deviation. SD. **p < 0.01. Full-length blots/gels are presented in Additional file 1

(See figure on next page.)

Fig. 4 Screening and validation of miR-92b-3p target gene USP28. **A,B** EKGG enrichment analysis on target genes of differentially expressed miRNAs in exosomes. **C** Two separate miRNA target databases were utilized for the prediction of potential miRNAs. **D** Identification of common target genes of miR-92b-3p. **E** Schematic representation of the *USP28* 3'-UTR, with mutations introduced at the predicted miR-92b-3p binding sites. **F** Comparative luciferase activity in HTR-8/SVneo cells co-transfected with MT-*USP28*-3'-UTR+miR-NC, MT-*USP28* 3'-UTR+miR-92b-3p mimics, WT-*USP28* 3'-UTR+miR-NC, or WT-*USP28* 3'-UTR+miR-92b-3p mimics. **G** Evaluation of *USP28* protein levels through WB in HTR-8/SVneo cells 48 h post-transfection with miR-92b-3p mimics or inhibitors. Error bars indicate standard deviation (SD). The results were obtained from six independent repetitions to ensure the reliability of the data. One-way ANOVA, Tukey's post hoc test, *** p < 0.001. Full-length blots/gels are presented in Additional file 1

Xiong et al. BMC Biology (2025) 23:222 Page 7 of 20

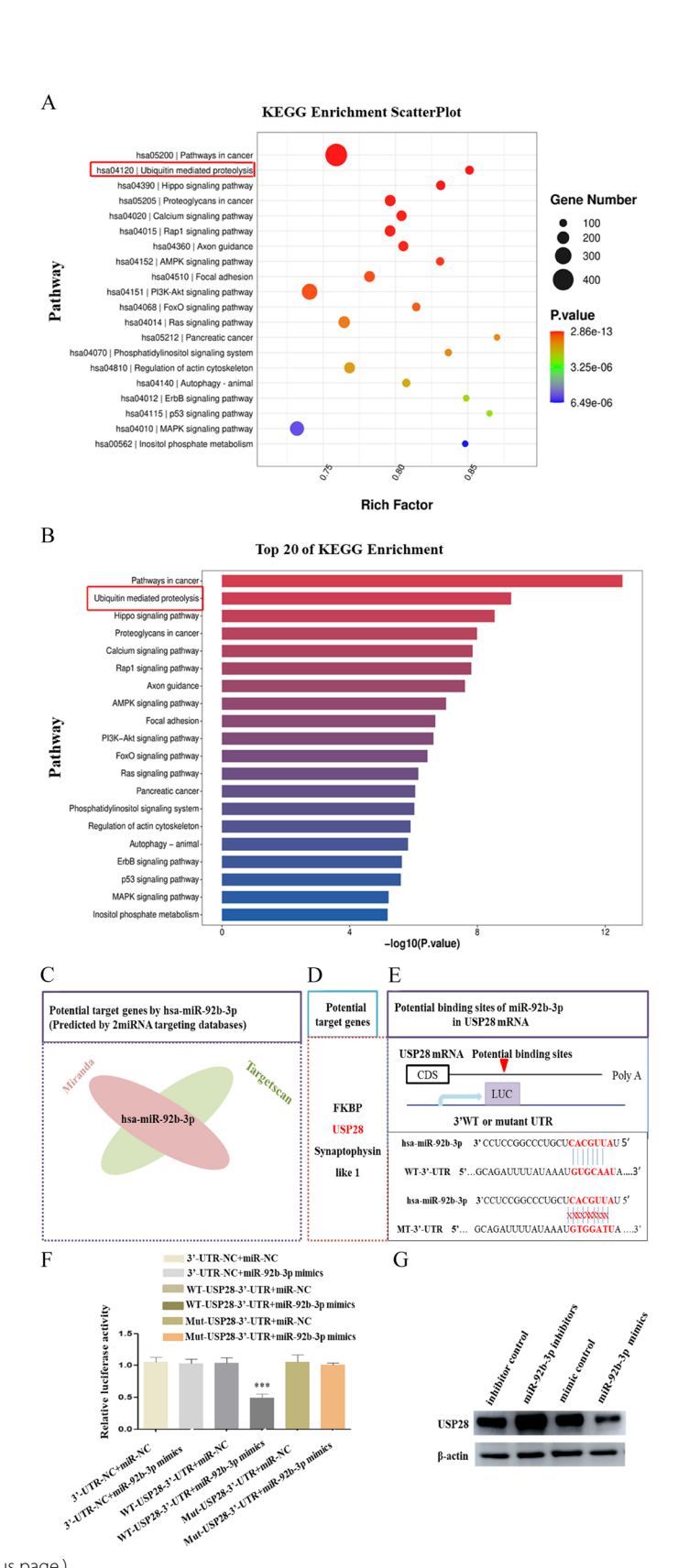


Fig. 4 (See legend on previous page.)

Xiong et al. BMC Biology (2025) 23:222 Page 8 of 20

miR-92b-3p suppresses EMT, migration, and invasion of trophoblasts by downregulating USP28 expression

The effect of USP28 on trophoblasts was investigated by transfection with siRNA targeting USP28 (si-USP28) or infection with adenovirus-USP28 (Ad-USP28). gRT-PCR and WB showed that in HTR-8/SVneo cells, si-USP28 decreased USP28 expression (1.02 ± 0.12), whereas Ad-USP28 increased the USP28 expression (4.02 ± 1.05) . In addition, Ad-USP28 infection resulted in upregulation of Snail and downregulation of E-cadherin at the protein level, whereas si-USP28 exerted an opposite effect on the expression of EMT-related molecules in HTR-8/SVneo cells (Fig. 5A,B and Additional file 1). Knockdown of USP28 significantly reduced the invasive and migratory capacities of HTR-8/SVneo cells, whereas overexpression of USP28 promoted these processes (Fig. 5C,D). In addition, Ad-USP28 counteracted the inhibitory effect of miR-92b-3p mimics on USP28 and Snail expression, while hindering the upregulation of E-cadherin induced by miR-92b-3p mimics in HTR-8/SVneo cells (Fig. 5E and Additional file 1). Co-transfection of Ad-USP28 reversed the restrictive effect of miR-92b-3p mimics on HTR-8/ SVneo cell invasion and migration (Fig. 5F,G). In conclusion, these findings suggest that exosomal miR-92b-3p may inhibit trophoblast EMT, migration, and invasion by directly suppressing USP28 expression.

URSA-DSC-exos promote embryo resorption rate by transferring miR-92b-3p

To investigate the role of DSC-exos in vivo, CBA/J female mice, mated with either BALB/c or DBA/2 male mice, were given injections of either URSA-DSC-exos, N-DSC-exos, or PBS through tail vein or intraperitoneal administration. The concentration of extracellular vesicle injection was gradually increased based on the results of in vitro cell experiments, as described in our previously reported method [43]. When the concentration reached 0.2 mg/mL, statistical differences were observed in in vivo experiments. The miR-92b-3p expression levels in the placenta were assessed using RT-PCR analysis.

The findings demonstrated that miR-92b-3p was overexpressed in mice treated with URSA-DSC-exos (Fig. 6A). Additionally, the administration of URSA-DSC-exos significantly increased the embryo resorption rate of normal pregnant mice, while N-DSC-exos led to a notable decrease in the embryo resorption rate of spontaneous abortion pregnant mice. Resorption rate was calculated as [(Number of total resorptions)/(Number of total implantations)] × 100%, as previously reported in our research [45]. Furthermore, adding the exosome inhibitor GW4869 to the culture medium of N-DSC and URSA-DSC can reverse the effect of N-DSC-exos and URSA-DSC-exos on the embryo resorption rate in spontaneous abortion pregnant mice (Fig. 6B,C). Furthermore, the USP28 expression level was significantly reduced in the placentas and uterine tissues of mice treated with URSA-DSC-exos (Fig. 6D and Additional file 1). Immunohistochemical staining revealed that USP28 was localized within the cell membrane and cytoplasm of both uterine and placental tissues (Fig. 6E). Collectively, the data supports the notion that URSA-DSC-exos contribute to an increased embryo resorption rate by transferring miR-92b-3p, which leads to the suppression of USP28 expression.

Expression of miR-92b-3p, USP28, and EMT-related molecules in the villi of URSA patients

In conclusion, our investigation focused on the expression levels of USP28 and miR-92b-3p in placenta villous tissues from 14 patients with URSA and 22 normal pregnant women. Our study revealed heightened expression levels of miR-92b-3p in samples derived from URSA patients, along with a reduction in USP28 expression at the protein level (Fig. 7A–C and Additional file 1). Immunohistochemistry and immunofluorescence were employed to assess the distribution of USP28, β -TrCP, E-cadherin, and Snail within the villi of patients with URSA. Notably, we observed diminished expression of USP28 and Snail in the villi of URSA patients compared to normal early pregnant women. In contrast, the

(See figure on next page.)

Fig. 5 miR-92b-3p suppresses EMT, migration, and invasion of trophoblasts by downregulating USP28 expression. **A,B** USP28, E-cadherin, Snail, N-cadherin, and Vimentin mRNA and protein levels were analyzed in HTR-8/SVneo cells 48 h post-transfection with si-*USP28* or Ad-*USP28* infection using qRT-PCR and WB techniques. **C,D** The migration and invasion abilities of HTR-8/SVneo cells transfected with si-*USP28* or infected with Ad-*USP28* were evaluated via wound healing and transwell assays, respectively. Representative images of migrated or invaded cells are displayed (magnification,×200). **E** Western blotting analysis was conducted on HTR-8/SVneo cells 72 h after transfection with miR-92b-3p mimic alone or in combination with Ad-*USP28* and miR-92b-3p mimics. **F** The migration capacities of HTR-8/SVneo cells transfected with miR-92b-3p mimics alone or in combination with Ad-*USP28* and miR-92b-3p mimics were assessed using wound healing. **G** The invasion capacities of HTR-8/SVneo cells transfected with miR-92b-3p mimics alone or in combination with Ad-*USP28* and miR-92b-3p mimics were assessed using transwell assays. Representative images of migrated or invaded cells are presented (magnification,×200). All experiments were repeated 6 times to ensure the accuracy of the data. Error bars indicate standard deviation. SD. One-way ANOVA, Tukey's post hoc test, **p < 0.01, **** p < 0.001. Full-length blots/gels are presented in Additional file 1

Xiong et al. BMC Biology (2025) 23:222 Page 9 of 20

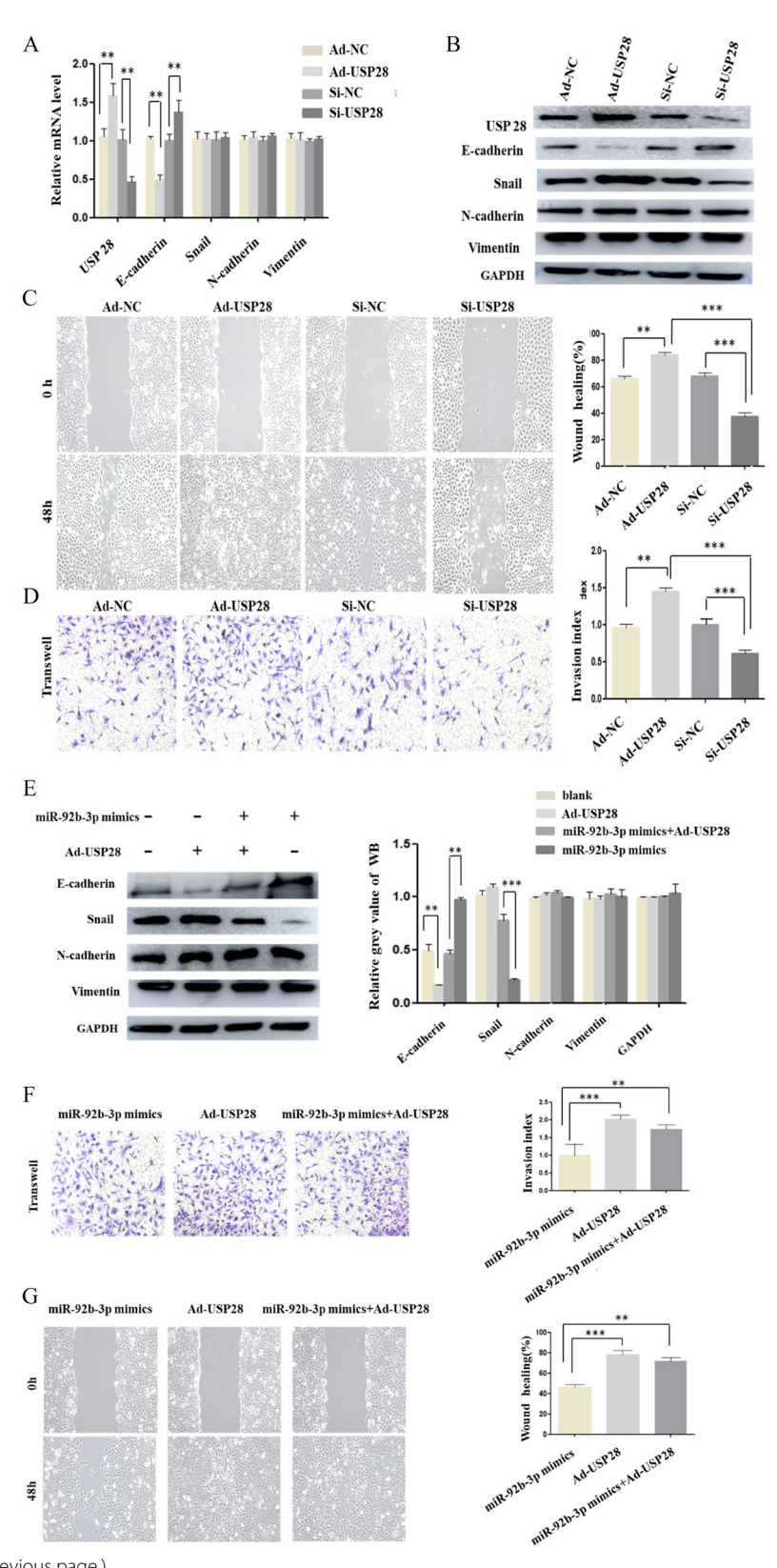


Fig. 5 (See legend on previous page.)

Xiong et al. BMC Biology (2025) 23:222 Page 10 of 20

expression levels of E-cadherin and β -TrCP were significantly increased (Fig. 7D,E). Collectively, these clinical observations supported the hypothesis that the upregulation of miR-92b-3p and downregulation USP28 may contribute to the insufficient migration and invasion of trophoblasts, potentially playing a critical role in the occurrence and development of URSA.

Discussion

Relevant studies have found that extracellular vesicles mediate the exchange of information between the embryo and the mother, and play a key role in pregnancy recognition, embryo implantation, immune regulation, embryo development, placenta formation, and labor [46-52]. Extracellular vesicles from the embryo, placenta, and maternal endometrium can influence pregnancy by delivering biological information such as proteins, lipids, mRNAs, and non-coding RNAs to recipient cells [53-59]. DSCs comprise approximately 70% of the cells at the maternal-fetal interface, and previous studies by our group [42, 60] have closely examined the metamorphosis of the endometrium, in which progesterone and estrogen play important roles in mediating EMT and metamorphosis of trophoblasts. Extracellular vesicles secreted by DSCs may be an important vehicle for establishing information transfer between them and trophoblasts. Impaired trophoblast invasion and migration functions have been found to be important causes of URSA [61, 62], and the EMT process plays a crucial role in these functions of trophoblasts [63]. Numerous studies have shown that EMT is an important step in trophoblast differentiation [64-66], occurring during trophoblast invasion. EMT dysregulation in trophoblasts has been associated with various pathological pregnancies [63, 65-68]. Our previous study showed that N-DSC-exos significantly increased the expression levels of the EMTrelated molecules Snail and N-cadherin in HTR-8/SVneo cells and decreased the mRNA and protein levels of E-cadherin [43]. Further studies revealed that the DSCexos-derived E3 ubiquitin ligase β-TrCP may mediate the ubiquitination degradation of Snail and regulate the stability of Snail proteins, thereby affecting EMT in trophoblasts [69].

In this study, miRNA mimics and inhibitors were used to further investigate the properties of trophoblasts, such as migration and invasion. It was found that USAR-DSC-exos-derived miR-22-5p_R-1 inhibited metabolic transformation of trophoblast cells by repressing the translation of the target gene PDK4, which appeared to be involved in trophoblast invasion and migration [43]. Interestingly, co-transfection of miR-92b-3p and miR-22-5p-R-1 mimics was more effective than transfection alone. Meanwhile, URSA-DSC-exos derived miR-22-5p_R-1 had no effect on the expression of Snail. Therefore, we speculated that the effect of URSA-DSCexos on the expression of Snail on trophoblast may be mediated by other mechanisms, suggesting that miR-92b-3p and miR-22-5p-R-1 may participate in regulating the invasion, migration, and EMT of trophoblasts through different mechanisms. Further, it was shown that miR-92b-3p mimics indeed inhibited the invasive and migratory abilities of HTR-8/SVneo cells in vitro and were accompanied by changes in EMT-related markers, including an increase in E-cadherin expression and a decrease in the levels of the transcription factor Snail protein. However, the expression of N-cadherin and Vimentin did not correlate with miR-92b-3p. Interestingly, although there was no statistically significant difference between the effects of miR-92b-3p mimics and inhibitors on the mRNA levels of the transcription factor Snail in HTR-8/SVneo cells, miR-92b-3p mimics significantly downregulated Snail protein expression compared to miR-92b-3p inhibitors. This inconsistency between Snail protein and mRNA levels is consistent with earlier findings, which hypothesized that excessive degradation of Snail proteins may be due to an abnormality in the E3 ubiquitin ligase β -TrCP. This raises the question: does miR-92b-3p cause abnormal expression of β-TrCP, thereby affecting Snail stability, or does it directly induce Snail protein degradation by inhibiting the expression of target genes? Further studies are needed to identify the target genes of miR-92b-3p and to determine through which target genes it regulates trophoblasts. In addition, we found that the average size of extracellular vesicles in URSA was smaller compared to that of normal gestational cells, which may be related to the abnormal metabolism of extracellular vesicles or apoptosis in URSA,

(See figure on next page.)

Fig. 6 URSA-DSC-exos promote embryo resorption rate by transferring miR-92b-3p. (A) Assessment of miR-92b-3p expression levels in the placenta of normal pregnany mouse model treated with URSA-DSC-exos on day 12 via qRT-PCR. **B,C** Embryo resorption rate in each group. **D** Quantification of USP28 protein expression in the placenta of normal pregnany mouse model treated with URSA-DSC-exos utilizing WB analysis. **E** Identification of USP28 distribution within the placenta and uterus by implementing immunohistochemistry (IHC) in the placenta and uters of normal pregnany mouse model treated with URSA-DSC-exos. Scale bars:×20;×40. Error bars, SD. One-way ANOVA, Tukey's post hoc test, **p < 0.01. Full-length blots/ qels are presented in Additional file 1

Xiong et al. BMC Biology (2025) 23:222 Page 11 of 20

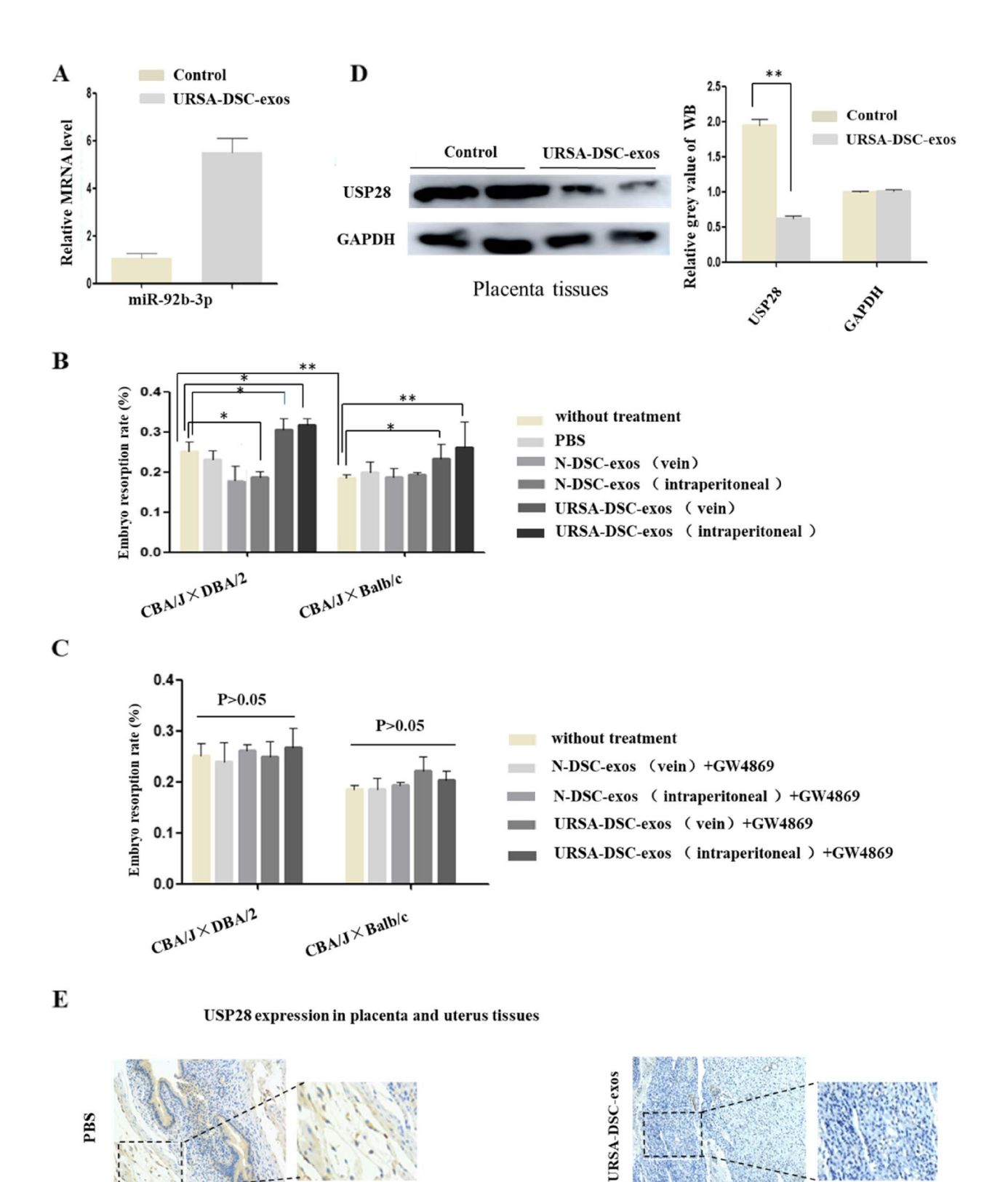


Fig. 6 (See legend on previous page.)

Xiong et al. BMC Biology (2025) 23:222 Page 12 of 20

affecting the generation and release of extracellular vesicles [70].

Combining relevant literature and preliminary research findings, we predicted that the target gene of miR-92b-3p is USP28. The protein USP28 is a member of the ubiquitin-specific protease (USP) family [70], which belongs to the deubiquitinating enzymes (DUBs), an essential component of the ubiquitin-proteasome pathway. Deubiquitinases can reverse the ubiquitination process, with the reverse process being catalyzed by DUBs. Contrary to the action of E1-E2-E3 ubiquitin ligases, DUBs can shorten or remove the ubiquitin chains from substrate proteins, thereby reversing the ubiquitination process [71]. As an important member of the DUB family, USP28 has been found to inhibit the EMT of tumor cells in the field of oncology [72]. Our research discovered that DSC-exos could regulate trophoblast invasion, migration, and EMT by controlling the E3 ubiquitin ligase β-TrCP-mediated degradation of Snail. Snail, as the most critical transcription factor of EMT, can be degraded through the ubiquitin-proteasome pathway mediated by β-TrCP, indicating it can be regulated by another class of factors involved in ubiquitination, namely deubiquitinases. Studies have found that the ubiquitination modification of substrates by E3 ubiquitin ligase can be reversed by deubiquitinases. DUBs can catalyze the hydrolysis of ubiquitin chains connected to substrate proteins, thus deubiquitinating the substrates and preventing their degradation by the proteasome [73]. USP28 influence the degradation of Snail protein through deubiquitination? What is the relationship between USP28 and the ubiquitin E3 ligase β-TrCP we discussed?

Based on the aforementioned research background, further studies were conducted, revealing that miR-92b-3p can bind to the 3'-UTR of *USP28*, thereby inhibiting the expression of the target gene *USP28*, leading to decreased stability of the Snail protein and ultimately affecting the EMT of trophoblast. However, the relationship between USP28, Snail, and β -TrCP is not yet clear. It has been found that deubiquitinases can regulate the EMT of tumors by deubiquitinating β -TrCP, thus controlling the stability of β -TrCP. It is possible that USP28 directly reverse the ubiquitination process of Snail by removing or shortening its ubiquitin chain, or it is possible that USP28 affected the

expression of Sanil protein by regulating β -TrCP. This will be the focus of our subsequent experiments to further clarify.

In vitro experiments have demonstrated that URSA-DSC-exos can suppress the invasion, migration, and EMT of trophoblast by delivering miR-92b-3p. This process effectively targets and inhibits the expression of miR-92b-3p target gene USP28, thereby inducing the excessive degradation of Snail. Then, it was found that the biological markers in clinical samples are consistent with the in vitro cell assay. In vitro experiments confirmed that N-DSC-exos significantly reduced the embryo resorption rate in the spontaneous abortion model mouse, whereas URSA-DSC-exos notably increased the embryo resorption rate in normal pregnant mouse model. This was accompanied by reduced expression of USP28 in the uterus and placental tissues of mice, aligning with the in vitro cell function experiment results. These findings from in vivo experiments further validate the results of the in vitro studies, suggesting that URSA-DSC-exos miR-92b-3p regulates USP28, thereby inhibiting the invasion, migration, and EMT of trophoblast.

This research indicates that DSC-exos play a crucial regulatory role in the proper differentiation of trophoblast and the EMT process. URSA-DSC-exos miR-92b-3p targets USP28, affecting the ubiquitin-proteasome system to regulate the degradation of Snail protein, thus inhibiting the invasion, migration, and EMT of trophoblasts. The differential expression of DSC-exos in URSA may explain the trophoblast differentiation disorders in URSA patients. These findings enrich our understanding of the physiological mechanisms of normal pregnancy and offer a novel perspective on the mechanisms underlying insufficient trophoblast differentiation in URSA. However, the differentiation of trophoblast and EMT is undoubtedly a process involving multiple factors. This study primarily focuses on the material exchange, information transmission, and functional regulation between DSC-exos at the maternal-fetal interface and trophoblast. Immune cells at the maternal-fetal interface and other factors may also participate in regulating the invasion, migration, and EMT of trophoblasts. The roles and mechanisms of these factors in the maternal-fetal interface microenvironment are worth further exploration.

(See figure on next page.)

Fig. 7 miR-92b-3p is upregulated in placental villous tissues from patients with URSA (n = 36, means \pm SD). **A** The expression levels of miR-92b-3p in placental villous tissues from patients with URSA (n = 14) and a control group (n = 22) was evaluated using qRT-PCR. **B, C** The expression levels of USP28 protein and mRNA in placental villous tissues of URSA patients via WB analysis and qRT-PCR, respectively. **D,E** IHC and IF were employed to investigate the distribution of USP28, E-cadherin, N-cadherin, and Snail within the placental villous tissues of URSA patients. Scale bars: \times 20; \times 40. Error bars, SD. One-way ANOVA, Tukey's post hoc test, **p< 0.01. Full-length blots/gels are presented in Additional file 1

Xiong et al. BMC Biology (2025) 23:222 Page 13 of 20

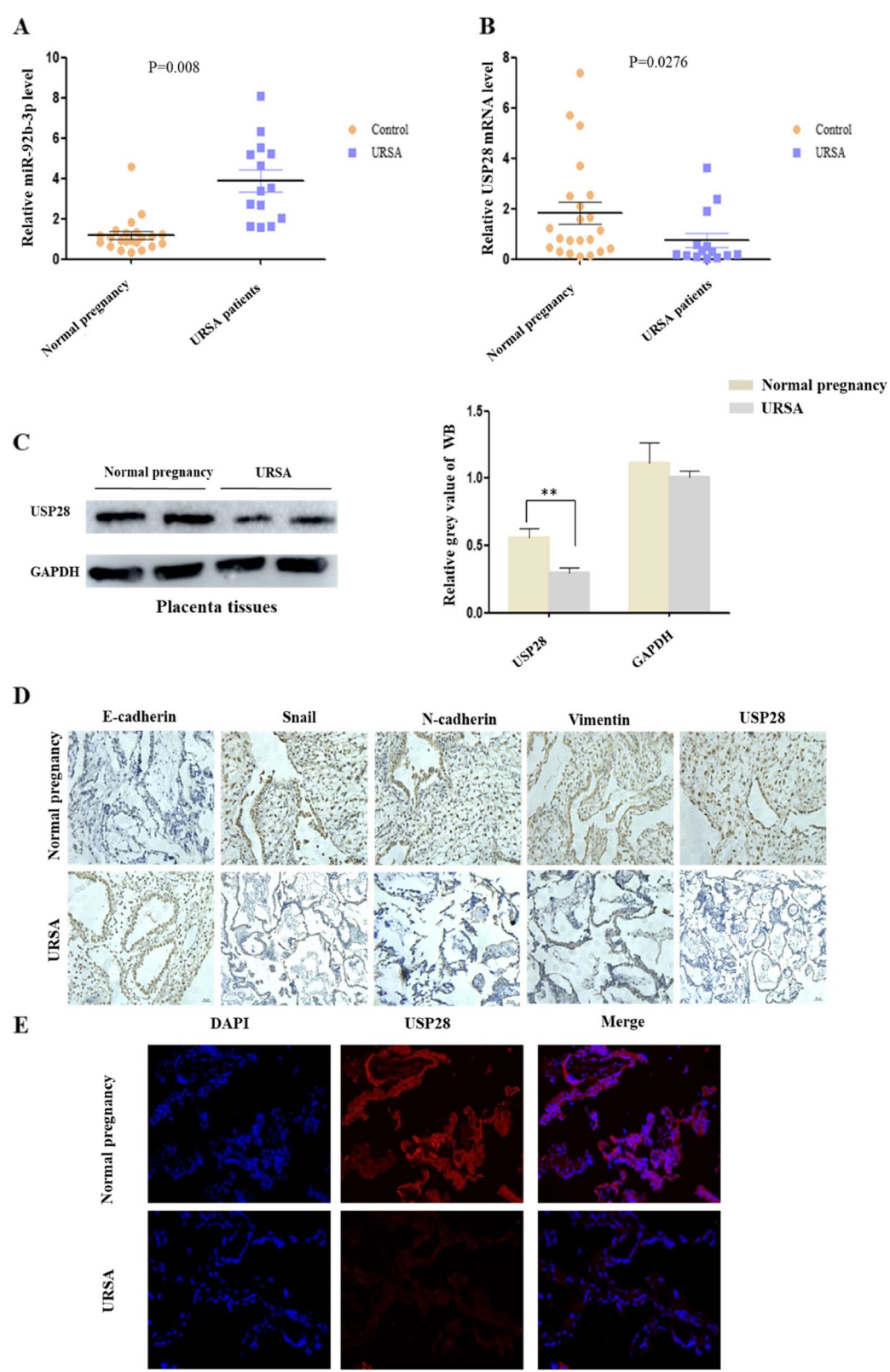


Fig. 7 (See legend on previous page.)

Xiong et al. BMC Biology (2025) 23:222 Page 14 of 20

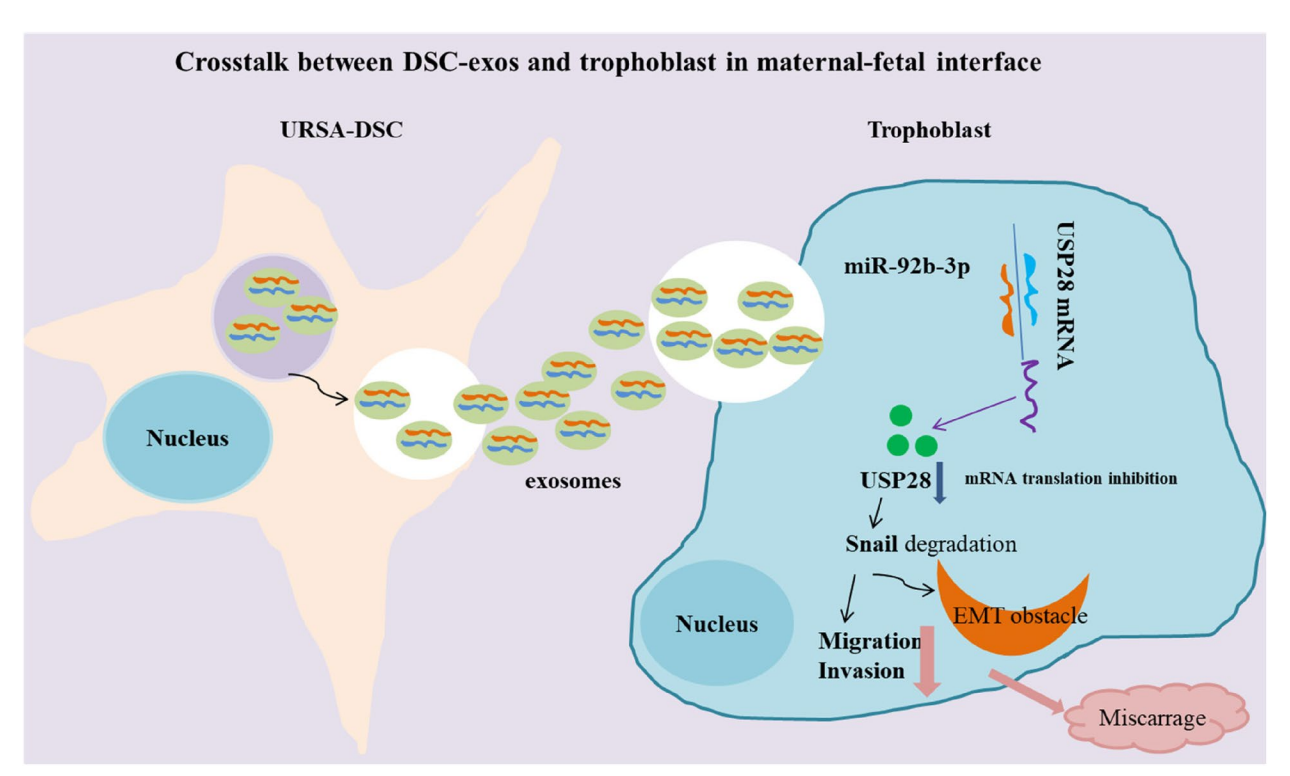


Fig. 8 Schematic illustration of URSA-DSC-derived miR-92b-3p inhibition of trophoblast EMT, migration, and invasion in URSA. Exosomes derived from DSC suppress EMT, migration, and invasion of trophoblasts by transporting miR-92b-3p to directly inhibit USP28 expression at the post-transcriptional level, thereby participating in the pathogenesis of URSA

Conclusions

In summary, our results show that URSA-DSC-exos suppress EMT, migration, and invasion of trophoblasts by transporting miR-92b-3p to inhibit USP28 expression at post-transcriptional level. This process induces abnormal ubiquitination and degradation of Snail, thereby contributing to the pathogenesis of URSA (Fig. 8). Further exploration of this process may illuminate novel regulatory mechanisms involving DSC and their influence on trophoblast function in the context of URSA.

Methods

Patients and tissue samples

Between September 2020 and December 2021, a total of 14 women with URSA, 22 women with normal pregnancies (NP), and 3 non-pregnant women participated in the study. URSA is defined as two or more consecutive spontaneous abortions for which no clear cause has been identified after detailed examination and evaluation. Inclusion criteria for the URSA group were as follows: (1) no uterine malformations; (2) absence or undetectability of a fetal heartbeat; (3) a history of two or more spontaneous abortions; (4) no endocrine,

metabolic, autoimmune diseases, thrombophilia, or infections; and (5) exclusion of chromosomal abnormalities in both parents and embryos. For the NP group, the presence of a fetal heartbeat was confirmed via ultrasound prior to elective pregnancy termination. Decidual tissues, collected during the 6 to 10 weeks gestation immediately following surgery under sterile conditions, were washed with cold phosphate-buffered saline (PBS) to remove blood and fetal tissue. Samples of these tissues was fixed in 4% paraformaldehyde for paraffin embedding. Three cases involved normal nonpregnant women with secretory endometrial tissue. The specimens were taken from patients who underwent surgical treatment for benign diseases in the gynecology department of our hospital. Inclusion criteria: (1) Age range from 22 to 40 years old; (2) Regular menstruation and surgery during the secretory phase; (3) No history of adverse pregnancy and childbirth; (4) No abnormalities or infections of the reproductive system; (5) No internal surgical complications, no endocrine system diseases; (6) No endometrial lesions, no endometriosis. All participants mentioned above were fully informed before signing the informed consent form. The baseline characteristics of the patients are presented in additional file 2:Tab.S1.

Xiong et al. BMC Biology (2025) 23:222 Page 15 of 20

Cell culture and reagents

The HTR-8/SVneo human trophoblast cell line was acquired from Yihe Biotechnology Co., Ltd (Shanghai, China). These cells were cultured in RPMI-1640 medium (Gibco, Grand Island, NY, USA) supplemented with 10% extracellular vesicle-free FBS (Gibco, Waltham, MA, USA) and maintained in a humidified environment with 5% CO₂ at 37 °C. This study adhered to strict aseptic culture techniques, assessed by microscopic observation, with a cell mortality rate of less than 1 in 10,000, ensuring there was no contamination of the in vitro tissue cultures. The concentration of extracellular vesicles used for the treatment of trophoblasts was approximately 200 vesicles/mL.

Isolation, culture, and identification of DSCs/ESCs

We performed negative pressure aspiration surgery to obtain decidual tissue samples from both normal pregnant women and URSA patients, ensuring no medication was administered to participants before or during the procedure. Decidual tissues were collected from gestational weeks 6 to 9. Subsequently, the DSCs/ESCs were isolated, cultured, and identificated as described in our previously reported method [42, 43]. The specificity of one of the primary antibodies was confirmed by peptide blocking assays.

Exosome isolation and treatment

Exosomes were collected from the supernatant of DSCs or ESCs (maintained in RPMI-1640 medium, supplemented with 10% exosome-free FBS) and isolated using ultracentrifugation, as described in our previously reported method [42, 43]. The protein content was assessed using the BCA protein assay kit (Beyotime, China). Approximately 20–30 µg of extracellular vesicles were procured from 10 ml of culture supernatant. The obtained extracellular vesicles were then employed to stimulate trophoblasts. HTR-8/SVneo cells were placed onto six-well plates, allowed to grow until reaching 50% confluence, and then treated with URSA-DSC-exos, N-DSC-exos, or N-ESC-exos. The cells were harvested for subsequent experiments after 48 h. In this study, extracellular vesicles were normalized by standardizing cell culture conditions and cell numbers, with an average of three extracellular vesicles per initial cell.

Exosome identification: TEM, NTA, and WB

We employed TEM, NTA, and WB to identify exsomes, as described in our previously reported method [43]. This study confirmed the absence of cellular contaminants by visualizing the morphology and size of extracellular vesicles by electron microscopy. The above methodology strictly follow the recommendations for extracellular

vesicles (EV) studies described in the MISEV2018 guidelines [44] to ensure the reliability and reproducibility of EV research.

Cellular internalization of exosomes

Initially, the PKH67 Green Fluorescent Cell Linker Kit (Sigma-Aldrich, USA) was used to label exosomes, as described in our previously reported method [43]. The labeled exosomes were resuspended in PBS and incubated with 60% confluent HTR-8/SVneo cells for 12, 24, and 48 h. Finally, the samples were examined and imaged with a laser confocal microscope. The specificity of one of the primary antibodies has been confirmed by peptide blocking assays.

Blockade of exosome generation

Inhibition of exosome release was achieved using GW4869 (Sigma-Aldrich). A concentration of 10 mM of GW4869 was introduced to the culture medium containing DSC along with 10% exosome-free FBS. After 48 h, the conditioned medium was collected for exosome isolation, following the previously outlined protocol.

miRNA sequencing of exosomes

The total RNA was extracted from URSA-DSC-exos and N-DSC-exos using the total RNA Isolation Kit (OBio, China). The quality and integrity of RNAs were assessed by agarose gel electrophoresis. The protocol for miRNA sequencing was described in our previously reported method [43]. Firstly, miRNA is reverse transcribed into cDNA, followed by the addition of adapter sequences, followed by PCR amplification and library construction. miRNAs were converted into sequencing libraries using specific kits (OBio, China). Then the constructed miRNA library was sequenced using the Illumin Hiseq platform to obtain the sequence information of miRNAs [43]. Finally, using miRNA data analysis software ACGT101 miRNA for analysis: (1) Obtain clean data: remove 3 'adapters and garbage sequences; (2) Length screening: Retain sequences with base lengths between 18 and 26 nt, and compare and analyze various RNA databases; (3) MiRNA identification: Obtain valid data and compare precursor and genome for miRNA identification; (4) Perform predictive analysis on target genes of differentially expressed miRNAs. This study used two software, Targeted Scan and miRanda, to predict target genes for significantly different miRNAs. The Raw sequencing data of miRNAs are deposited in Database (Genome Sequence Archive) with the identifer HRA011381.

Cell transfection

MicroRNA mimics and inhibitors for miRNA-92b-3p, small interfering RNA (siRNA) targeting USP28, and

Xiong et al. BMC Biology (2025) 23:222 Page 16 of 20

relevant primers were obtained from Shanghai GenePharma. The mimic control, inhibitor control, and siRNA-control targeting USP28 from Shanghai GenePharma served as control groups for the experiment, with the mock control group acting a negative control. Adenovirus for USP28 overexpression (Ad-USP28) and a negative control were also sourced from Shanghai GenePharma (China). Infections of adenovirus were conducted when cell confluence reached 60-70%. HTR-8/SVneo cells were seeded onto 6-well plates 24 h prior to transfection. Once the HTR-8/SVneo cells attained 50-60% confluence, miRNA-92b-3p mimics or miRNA-92b-3p inhibitors were transfected using Lipofectamine 2000 (Invitrogen, USA), following the manufacturer's protocol. Transfection with siRNA targeting USP28 was carried out using RFect siRNA Transfection Reagent (Baidai Biotechnology Co., Ltd, Changzhou, China). Cells were collected for subsequent experiments 48 h post-transfection. For Ad-*USP28* infections, HTR-8/SVneo cells were incubated with polybrene (Shanghai GenePharma, China) when cell confluence reached 40-50%. Cells were harvested for further analysis 48–72 h post-infection.

RNA isolation and quantitative real-time PCR (qRT-PCR)

Total RNA of exosomes or HTR-8/SVneo cells subjected to different treatments was extracted using the TRIzol Reagent (Beyotime, Shanghai) following the manufacturer's guidelines. For both mRNA and miRNA expression analysis, cDNA was synthesized using the mRNA Reverse-Transcription Kit (Beyotime, Shanghai). Quantitative assays were performed using the SYBR Green PCR Mix (Vazyme Biotech, Shanghai) with a Real-Time PCR System. The relative mRNA and miRNA expression levels were calculated using the $2-\Delta\Delta Ct$ method. miRNA primers were supplied by Sangon Biotech (Shanghai), and the sequences of the primers are provided in additional file 2:Tab.S2. All of the aforementioned methods follow the MIQE guidelines.

Western blotting

Protein extraction from HTR-8/SVneo cells was performed using RIPA lysis buffer (Beyotime, Jiangsu, China), and the protein concentration of each extract was measured using a BCA Kit (Beyotime, Jiangsu, China) according to the manufacturer's protocol. WB were employed to detect the expression of these proteins in the trophoblast, including N-cadherin, E-cadherin, USP28,Vimentin, and Snail, with GAPDH and β -actin as internal reference, as described in our previously reported method [43].

Transwell assay and wound healing assay

Transwell assay and wound healing assay were performed to evaluate the invasion and migration potential of HTR-8/SVneo cells. The detailed experimental steps were described in our previous research [42, 43]. HTR-8/SVneo cells co-cultured with exosomes at a concentrations of 20 μ g/mL. The above experiments were analyzed in a blinded manner.

Dual-luciferase reporter assay

The 3'-UTR sequence of the USP28 gene (wild-type 3'-UTR) and the binding sites for miR-92b-3p were amplified and subsequently sub-cloned into the p-MIRreporter plasmid (OBIO Technology Co., Ltd, Shanghai, China). The wild-type 3'-UTR of USP28, containing the mutant miR-92b-3p binding site sequences, was altered (from GUGCAAU to GTGGATU, mut-3'-UTR) and integrated into a corresponding luciferase reporter plasmid. HTR-8/SVneo cells were co-transfected with the mutant or wild-type 3'-UTR reporter and miR-92b-3p mimics (OBIO technology, Shanghai, China). The Renilla luciferase reporter vector Prl-SV40 (Promega, USA) was utilized as an internal transfection control. After 48 h of transfection, total cell lysates were collected, and the luciferase activity of Renilla was assessed using the Dual-Luciferase Reporter Assay System according to the manufacturer's guidelines. A total of six biological replicates were evaluated in this trial.

Immunohistochemistry

Villus samples from healthy pregnant women (22 cases) and URSA patients (14 cases) were collected between 6 and 10 weeks of gestation. These samples were fixed in a 10% formalin solution and subsequently embedded in paraffin blocks. Immunohistochemistry was employed to detect the expression of these proteins in the Villus, including N-cadherin, E-cadherin, USP28, Vimentin, and Snail, as described in our previously reported method [43]. All the antibodies information are presented in additional file 2:Tab.S3.

Immunofluorescence

Fresh uterine and placental tissues were obtained from pregnant mice and fixed with 4% paraformaldehyde for 12 h. Subsequently, the tissues were embedded in paraffin and cut into 4-micron-thick sections. The sections were baked at 60 °C for 30 min. First, the sections were immersed in xylene for 10 min, and this process was repeated three times. Then, the sections were sequentially placed in 100%, 95%, 85%, and 75% ethanol solutions, with each concentration being soaked for 5 min. After that, the sections were rinsed with distilled water

Xiong et al. BMC Biology (2025) 23:222 Page 17 of 20

for 5 min. The sections were soaked in citrate buffer and then heated at high power in a microwave for 8 min until they cooled to room temperature. After cooling, the sections were washed with PBS for 3 min, and this step was repeated three times. At room temperature, 3% hydrogen peroxide was added for 10 min to inactivate endogenous enzymes, and then the sections were rinsed with PBS for 3 min, repeating this process three times. The sections were placed in a wet box, and serum was added at room temperature for 20 min. The diluted primary antibody was added dropwise and incubated overnight in a 4 °C refrigerator. The sections were washed with PBS three times, each for 3 min. After removing the excess liquid on the sections, the diluted fluorescent secondary antibody was added. The sections were incubated in the dark at 37 °C in a wet box for 1 h, and then washed with PBS three times. The sections were incubated with DAPI in the dark for 5 min, and then rinsed with PBS four times to remove the excess DAPI. The sections were sealed with anti-fluorescence quenching sealing agent and observed under a fluorescence microscope. All antibody information is shown in additional file 3:Tab.S3.

Animal experiments

A spontaneous abortion mouse model and a normal pregnancy mouse model were established using 6-8-week-old male Balb/c, male DBA/2, and female CBA/J mice, provided by Huafukang Biotechnology Co., Ltd (Beijing, China). The normal pregnancy mouse model $(CBA/J \times Balb/c)$ and the spontaneous abortion mouse model (CBA/J×DBA/2) were used in this study. Each female mouse was injected with N-DSC-exos or URSA-DSC-exos (0.2 mg/mL) or PBS via tail vein on the day of implantation detection (day 1), three consecutive days prior to mating, and three consecutive days after conception (once per day). Pregnant mice were euthanized through cervical dislocation on days 12-14, their uteri were extracted, and the total number of implantation and resorption sites (indicative of abortion) were recorded, as previously reported in our research [45]. The embryo resorption rate was calculated as [(Number of total resorptions)/(Number of total implantations)] × 100%. To further determine the effect of the exosomes on the embryo resorption rate of pregnant mice, we added the exosome inhibitor GW4869 to an equal number of N-DSC and URSA-DSC culture medium. We then injected the extracted exosomes into the pregnant mice via the tail vein and abdominal cavity to observe the changes in embryo resorption rate. In this study, we confirmed that the results were not affected by genetic variation using the Balb/c×Balb/c hybridization technique, and the result is shown in additional file 2:Fig.S1.

Statistical analysis

All experiments were conducted a minimum of three times. All data were checked and verified for normal distribution using the Shapiro–Wilk test and for homogeneity of variances using Levene's test. Statistical evaluations were completed using GraphPad Prism 5 software. The findings are presented as mean±standard deviation (SD), and graphical representations of the collected data were created using GraphPad Prism 5 software. To assess the significance of differences between two groups, a two-tailed unpaired Student's *t* test was used, while a one-way ANOVA was employed for comparing three or more groups. For multiple group comparisons, a one-way ANOVA followed by Tukey's post hoc test was utilized. A *p*-value of < 0.05 was considered statistically significant.

Abbreviations

BSA Bovine serum albumin CTB Cytotrophoblast DSC Decidual stromal cell

DSC-exos Exosomes derived from decidual stromal cells ESC-exos Exosomes derived from endometrial stromal cells

Exos Exosomes E-Cad E-Cadherin

EMT Epithelial-mesenchymal transformation

FSC Endometrial stromal cells EVs Extracellular vesicles **EVT** Extravillous trophablast FRS Fetal bovine serum **FGR** Fetal growth restriction **GDM** Gestational diabetes mellitus Immunohistochemistry ΙH NTA Nanoparticle Tracking Analysis

N-cad N-cadherin

PDK4 Pyruvate dehydrogenase kinase 4

PE Preeclampsia

qRT-PCR Quantitative real-time polymerase chain reaction

RSA Recurrent spontaneous abortion RISC RNA-induced silencing complex

SD Standard deviation STB Syncytiotrophoblast

TEM Transmission electron microscopy

URSA Unexplained recurrent spontaneous abortion

WB Western blot

Supplementary Information

The online version contains supplementary material available at https://doi.org/10.1186/s12915-025-02326-4.

Additional file 1. Images of the original, uncropped gels/blots.

Additional file 2: Tab.S1.The characteristics of included study population. Tab.S2. The primers information used in this study. Tab.S3. Antibody information, cell line information and software information. Fig.S1. The embryo resorption rate between the Balb/c×Balb/c and CBA/2×Balb/c groups.

Acknowledgements

The authors express their gratitude to the Department of Obstetrics and Gynecology at Renji Hospital for their involvement in this research.

Authors' contributions

XMamethodology, formal analysis, original draft preparation, writing and editing, project administration, funding acquisition; HZQitormal analysis,

Xiong et al. BMC Biology (2025) 23:222 Page 18 of 20

investigation, data curation, project administration; WLPstoftware, validation, resources, visualization; ZAM—data curation, review and editing, supervision, funding acquisition. All authors read and approved the final manuscript.

Authors' information

The information of authors are available within the article.

Funding

This research received financial assistance from the National Natural Science Foundation of China (Grant Nos. 81671481 and 81871179), as well as from the Shanghai Pudong New Area Science and Technology Commission (Grant No. PKJ2021-Y51) and the College level project of the Sixth People's Hospital Affiliated to Shanghai Jiao Tong University School of Medicine (Grant No.ynhglg202413 and ynhg202211).

Data availability

All data generated or analyzed during this study are included in this published article, its supplementary information files, and publicly available repositories. The raw sequence data reported in this paper have been deposited in the Genome Sequence Archive (Genomics, Proteomics & Bioinformatics 2021) in National Genomics Data Center [74, 75] (Nucleic Acids Res 2022), China National Center for Bioinformation/Beijing Institute of Genomics, Chinese Academy of Sciences (GSA-Human: HRA011381) that are publicly accessible at https://ngdc.cncb.ac.cn/gsa-human. Uncropped Western blots are provided in Additional fle 1.

Declarations

Ethics approval and consent to participate

The tissue specimens employed in this research were procured after informed consent was obtained, which was approved by the Ethics Committee of Renji Hospital affiliated to Shanghai Jiaotong University, and the ethical Number: RA-2020–063. The animals used in this study were approved by the Ethics Committee of the Sixth People's Hospital affiliated to Shanghai Jiaotong University, and the ethical Number: 2022–0056.

Consent for publication

All authors agree to publish in the journal.

Competing interests

The authors declare that they have no competing interests.

Author details

¹Department of Obstetrics and Gynecology, Shanghai Sixth People's Hospital Affiliated to Shanghai Jiao Tong University School of Medicine, Shanghai, China. ²Department of Obstetrics and Gynecology, Renji Hospital, School of Medicine, Shanghai Jiao Tong University, 160 Pu Jian Road, Shanghai 200127, China.

Received: 24 November 2023 Accepted: 7 July 2025 Published online: 22 July 2025

References

- Cindrova-Davies T, Sferruzzi-Perri AN. Human placental development and function. Semin Cell Dev Biol. 2022;131:66–77.
- Lijin P, Weijie Z, Yin Tingxuan Xu, Chunfang WG, Meirong Du. The unique expression pattern of human leukocyte antigen in trophoblasts potentially explains the key mechanism of maternal-fetal tolerance and successful pregnancy. J Reprod Immunol. 2023. https://doi.org/10.1016/j. iri 2023.103880
- Staff AC, Fjeldstad HE, Fosheim IK, Moe K, Turowski G, Johnsen GM, et al.
 Failure of physiological transformation and spiral artery atherosis: their
 roles in preeclampsia. Am J Obstet Gynecol. 2022;226(2):S895–906.
- Lyall F, Robson SC, Bulmer JN. Spiral artery remodeling and trophoblast invasion in preeclampsia and fetal growth restriction: relationship to clinical outcome. Hypertension. 2013;62(6):1046–54.

- Deepak V, Ravikumar N, Badell ML, Sidell N, Rajakumar A. Transcription factor ID1 is involved in decidualization of stromal cells: implications in preeclampsia. Pregnancy Hypertension. 2020;21:7–13.
- Abbas Y, Turco MY, Burton GJ, Moffett A. Investigation of human trophoblast invasion in vitro. Hum Reprod Update. 2020;26(4):501–13.
- Pijnenborg R. Trophoblast invasion. Reproductive Medicine Review. 1994;3(1):53–73.
- Anin S, Vince G, Quenby S. Trophoblast invasion. Hum Fertil. 2004;7(3):169–74.
- Zhu H, Hou CC, Luo LF, Hu YJ, Yang WX. Endometrial stromal cells and decidualized stromal cells: origins, transformation and functions. Gene. 2014:551(1):1–14.
- Dos Santos E, Moindjie H, Sérazin V, Arnould L, Rodriguez Y, Fathallah K, et al. Preimplantation factor modulates trophoblastic invasion throughout the decidualization of human endometrial stromal cells. Reprod Biol Endocrinol. 2021;19:1–11.
- 11. Murata H, Tanaka S, Okada H. The regulators of human endometrial stromal cell decidualization. Biomolecules. 2022;12(9):1275.
- 12. Tang B, Guller S, Gurpide E. Mechanisms involved in the decidualization of human endometrial stromal cells. Acta Eur Fertil. 1993;24(5):221–3.
- Qiu Q, Li Y, Fong SW, Lee KC, Chen ACH, Ruan H, et al. Endometrial stromal cells from women with repeated implantation failure display impaired invasion towards trophoblastic spheroids. Reproduction. 2023;165(3):335–46.
- Goudarzi ST, Vousooghi N, Verdi J, Mehdizadeh A, Aslanian-Kalkhoran L, Yousefi M, et al. Autophagy genes and signaling pathways in endometrial decidualization and pregnancy complications. J Reprod Immunol. 2024. https://doi.org/10.1016/j.jri.2024.104223.
- Ander SE, Diamond MS, Coyne CB. Immune responses at the maternalfetal interface. Sci Immunol. 2019. https://doi.org/10.1126/sciimmunol. aat6114.
- Bansal AS. Joining the immunological dots in recurrent miscarriage. Am J Reprod Immunol. 2010;64(5):307–15.
- Warning JC, McCracken SA, Morris JM. A balancing act: mechanisms by which the fetus avoids rejection by the maternal immune system. Reproduction. 2011;141(6):715–24.
- 18. Zhang S, Xiao Yi, Wang Y, Qian C, Zhang R, Liu J. Role of kisspeptin in decidualization and unexplained recurrent spontaneous abortion via the ERK1/2 signalling pathway. Placenta. 2023;133:1–9.
- Sahu MB, Deepak V, Gonzales SK, Rimawi B, Watkins KK, Smith AK, et al. Decidual cells from women with preeclampsia exhibit inadequate decidualization and reduced sFlt1 suppression. Pregnancy Hypertens. 2019:15:64–71.
- Sun C, Groom KM, Oyston C, Chamley LW, Clark AR, James JL. The placenta in fetal growth restriction: what is going wrong? Placenta. 2020;96:10–8.
- Wang J, Ding J, Zhang S, Chen X, Yan S, Zhang Y, et al. Decreased USP2a expression inhibits trophoblast invasion and associates with recurrent miscarriage. Front Immunol. 2021. https://doi.org/10.3389/fimmu.2021. 717370.
- 22. Ford HB, Schust DJ. Recurrent pregnancy loss: etiology, diagnosis, and therapy. Rev Obstet Gynecol. 2009;2(2):76–83.
- Definitions of infertility and recurrent pregnancy loss. a committee opinion. Fertil Steril. 2013;99(1):63.
- El Hachem H, Crepaux V, May-Panloup P, Descamps P, Legendre G, Bouet PE. Recurrent pregnancy loss: current perspectives. Int J Womens Health. 2017;9:331–45.
- 25. Garrido-Gimenez C, Alijotas-Reig J. Recurrent miscarriage: causes, evaluation and management. Postgrad Med J. 2015;91(1073):151–62.
- 26. Rai R, Regan L. Recurrent miscarriage. Lancet. 2006;368(9535):601–11.
- 27. Pijnenborg R, Vercruysse L, Hanssens M. The uterine spiral arteries in human pregnancy: facts and controversies. Placenta. 2006:27(9–10):939–58.
- Illsley NP, DaSilva-Arnold SC, Zamudio S, Alvarez M, Al-Khan A. Trophoblast invasion: Lessons from abnormally invasive placenta (placenta accreta). Placenta. 2020;102:61–6.
- Hannon T, Innes BA, Lash GE, Bulmer JN, Robson SC. Effects of local decidua on trophoblast invasion and spiral artery remodeling in focal placenta creta-an immunohistochemical study. Placenta. 2012;33(12):998–1004.

- Winship A, Correia J, Krishnan T, Menkhorst E, Cuman C, Zhang J-G. Blocking Endogenous Leukemia Inhibitory Factor During Placental Development in Mice Leads to Abnormal Placentation and Pregnancy Loss. Sci Rep. 2015. https://doi.org/10.1038/srep13237.
- Natenzon A, McFadden P, DaSilva-Arnold SC, Zamudio S, Illsley NP. Diminished trophoblast differentiation in early onset preeclampsia. Placenta. 2022;120:25–31.
- Mohr AM, Mott JL. Overview of MicroRNA Biology. Semin Liver Dis. 2015;35(01):003–11.
- Ambros V. The function of animal MicroRNAs. Nature. 2004;431(7006):350–5.
- 34. Sayed D, Abdellatif M. MicroRNAs in development and disease. Physiol Rev. 2011;91(3):827–87.
- 35. Lewis BP, Burge CB, Bartel DP. Conserved seed pairing, often flanked by adenosines, indicates that thousands of human genes are microRNA targets. Cell. 2005;120(1):15.
- Salomon C, Rice GE. Role of Exosomes in Placental Homeostasis and Pregnancy Disorders. Prog Mol Biol Transl Sci. 2017;145:163–79.
- Lv C, Wen-Xian Yu, Wang Y, Yi D-J, Zeng M-H, Xiao H-M. MicroRNA-21 in extracellular vesicles contributes to the growth of fertilized eggs and embryo development in mice. Biosci Rep. 2018. https://doi.org/10.1042/ BSR20180036.
- 38. Zhang Y, Zhou J, Li M-Q, Xu J, Zhang J-P, Jin L-P. MicroRNA-184 promotes apoptosis of trophoblast cells via targeting WIG1 and induces early spontaneous abortion. Cell death & disease. 2019;10(3):223.
- Oghbaei F, Zarezadeh R, Jafari-Gharabaghlou D, Ranjbar M, Nouri M, Fattahi A, et al. Epithelial-mesenchymal transition process during embryo implantation. Cell Tissue Res. 2022;388(1):1–17.
- Choudhury J, Pandey D, Chaturvedi PK, Gupta S, et al. Epigenetic regulation of epithelial to mesenchymal transition: a trophoblast perspective. Mol Hum Reprod. 2022. https://doi.org/10.1093/molehr/gaac013.
- 41. Vićovac L, Aplin JD. Epithelial-mesenchymal transition during trophoblast differentiation. Cells Tissues Organs. 1996;156(3):202–16.
- Chen C, Li C, Liu W, Guo F, Kou X, Sun S, et al. Estrogen-induced FOS like 1 regulates matrix metalloproteinase expression and the motility of human endometrial/decidual stromal cells. J Biol Chem. 2020;295(8):2248–58.
- 43. Xiong M, Li Li, Wen L, Zhao A. Decidual stromal cell–derived exosomes deliver miR-22-5p_R-1 to suppress trophoblast metabolic switching from mitochondrial respiration to glycolysis by targeting PDK4 in unexplained recurrent spontaneous abortion. Placenta. 2024;153:1–21.
- 44. Théry C, Witwer KW, Aikawa E, Alcaraz MJ, Anderson JD, Andriantsitohaina R, et al. Minimal information for studies of extracellular vesicles 2018 (MISEV2018): a position statement of the International Society for Extracellular Vesicles and update of the MISEV2014 guidelines. J Extracell Vesicles. 2018. https://doi.org/10.1080/20013078.2018.1535750.
- Xiong M, Jihong Lu, Zhao A, Liang Xu, Bao S, Lin Q, et al. Therapy with Fasl-gene–modified dendritic cells confers a protective microenvironment in murine pregnancy. Fertil Steril. 2010;93(8):2767–9.
- Vilella F, Moreno-Moya JM, Balaguer N, Grasso A, Herrero M, Martínez S, et al. Hsa-miR-30d, secreted by the human endometrium, is taken up by the pre-implantation embryo and might modify its transcriptome. Development. 2015;142(18):3210–21.
- Balaguer N, Moreno I, Herrero M, Gonzalez M, Simon C, Vilella F. Heterogeneous nuclear ribonucleoprotein CI may control miR-30d levels in endometrial exosomes affecting early embryo implantation. Mol Human Reprod. 2018:24(8):411–25.
- Zhao G, Yang C, Yang J, Liu P, Jiang K, Shaukat A, et al. Placental exosomemediated Bta-miR-499-Lin28B/let-7 axis regulates inflammatory bias during early pregnancy. Cell Death Dis. 2018;9(6):704.
- 49. Ruiz-González I, Xu J, Wang X, Burghardt RC, Dunlap KA, Bazer FW, et al. Exosomes, endogenous retroviruses and toll-like receptors: pregnancy recognition in ewes. Reproduction. 2015;149(3):281–91.
- Bidarimath M, Khalaj K, Kridli RT, Kan FWK, Koti M, Tayade C. Extracellular vesicle mediated intercellular communication at the porcine maternalfetal interface: A new paradigm for conceptus-endometrial cross-talk. Rep. 2017; https://doi.org/10.1038/srep40476.
- Giacomini E, Vago R, Sanchez AM, Podini P, Zarovni N, Murdica V, et al. Secretome of in vitro cultured human embryos contains extracellular vesicles that are uptaken by the maternal side. Scientific Reports. 2017;7(1):5210.

- Ng YH, Rome S, Jalabert A, Forterre A, Singh H, Hincks CL, et al. Endometrial Exosomes/Microvesicles in the Uterine Microenvironment: A New Paradigm for Embryo-Endometrial Cross Talk at Implantation. Plos One. 2013. https://doi.org/10.1371/journal.pone.0058502.
- Ander SE, Diamond MS, Coyne CB. Immune responses at the maternalfetal interface. Science Immunolog. 2019. https://doi.org/10.1126/sciim munol.aat6114.
- Warning JC, Mccracken SA. A balancing act: mechanisms by which the fetus avoids rejection by the maternal immune system. Reproduction. 2011;141(6):715.
- Baig S, Lim JY, Fernandis AZ, Wenk MR, Kale A, Su LL, et al. Lipidomic analysis of human placental Syncytiotrophoblast microvesicles in adverse pregnancy outcomes. Placenta. 2013;34(5):436–42.
- 56. Vargas A, Zhou S, Éthier-Chiasson M, Flipo D, Lafond J, Gilbert C, et al. Syncytin proteins incorporated in placenta exosomes are important for cell uptake and show variation in abundance in serum exosomes from patients with preeclampsia. Faseb Journal Official Publication of the Federation of American Societies for Experimental Biology. 2014;28(8):3703–19.
- Salomon C, Yee SW, Mitchell MD, Rice GE. The Possible Role of Extravillous Trophoblast-Derived Exosomes on the Uterine Spiral Arterial Remodeling under Both Normal and Pathological Conditions. Biomed Research International. 2014. https://doi.org/10.1155/2014/693157.
- Wu L, Zhou H, Lin H, Qi J, Zhu C, Gao Z, et al. Circulating microRNAs are elevated in plasma from severe preeclamptic pregnancies. Reproduction. 2012;143(3):389–97.
- Rusterholz C, Hahn S, Holzgreve W. Role of placentally produced inflammatory and regulatory cytokines in pregnancy and the etiology of preeclampsia. Seminars in Immunopathology. 2007;29(2):151–62.
- Chen C, Kang X, Li C, Guo F, Wang Q, Zhao A. Involvement of signal transducers and activators of transcription in trophoblast differentiation. Placenta. 2021;105(2):94–103.
- Ding J, Cheng Y, Zhang Y, Liao S, Yin T, Yang J. The miR-27a-3p/USP25 axis participates in the pathogenesis of recurrent miscarriage by inhibiting trophoblast migration and invasion. J Cell Physiol. 2019;234(11):19951–63.
- Tian F-J, Qin C-M, Li X-C, Fan Wu, Liu X-R, Wang-Ming Xu, et al. Decreased Stathmin-1 Expression Inhibits Trophoblast Proliferation and Invasion and Is Associated with Recurrent Miscarriage. Am J Pathol. 2015;185(10):2709–21.
- 63. Kokkinos MI, Murthi P, Wafai R, Thompson EW, Newgreen DF. Cadherins in the human placenta–epithelial–mesenchymal transition (EMT) and placental development. Placenta. 2010;31(9):747–55.
- 64. Martin KF, Jürgen P. Human placental trophoblast invasion and differentiation: a particular focus on Wnt signaling. Front Genet. 2013;4:190.
- Davies JE, Pollheimer J, Yong HE, Kokkinos MI, Kalionis B, et al. Epithelialmesenchymal transition during extravillous trophoblast differentiation. Cell Adh Migr. 2016;10(3):310–21.
- Jordan NV, Johnson GL, Abell AN. Tracking the intermediate stages of epithelial-mesenchymal transition in epithelial stem cells and cancer. Cell Cycle. 2011;10(17):2865–73.
- Blechschmidt K, Mylonas I, Mayr D, Schiessl B, Schulze S, Becker K-F, et al. Expression of E-cadherin and its repressor snail in placental tissue of normal, preeclamptic and HELLP pregnancies. Virchows Arch. 2007;450(2):195–202.
- 68. Zhang D, Liu H, Zeng Ji, Miao X, Huang W, Chen H, et al. Glucocorticoid exposure in early placentation induces preeclampsia in rats via interfering trophoblast development. Gen Comp Endocrinol. 2016;225:61–70.
- Xiong M, Wang Q, Zhang X, Wen L, Zhao A, et al. Decidual stromal cells-derived exosomes incurred insufficient migration and invasion of trophoblast by disturbing of β-TrCP-mediated snail ubiquitination and degradation in unexplained recurrent spontaneous abortion. Eur J Med Res. 2024;29(1):39.
- Schubert U, Antón LC, Gibbs J, Norbury CC, Yewdell JW, Bennink JR. Rapid degradation of a large fraction of newly synthesized proteins by proteasomes. Nature. 2000;404(6779):770–4.
- 71. Clague MJ, Urbe S, Komander D. Breaking the chains: structure and function of the deubiquitinases. Cell Biology. 2009;10(8):550–63.
- Chen B, Sang Y, Song X, Zhang D, Wang L, Zhao W, et al. Exosomal miR-500a-5p derived from cancer-associated fibroblasts promotes breast cancer cell proliferation and metastasis through targeting USP28. Theranostics. 2021;11(8):3932–47.

Xiong et al. BMC Biology (2025) 23:222 Page 20 of 20

 D'Arcy P, Brnjic S, Olofsson MH, Fryknäs M, Lindsten K, De Cesare M, et al. Inhibition of proteasome deubiquitinating activity as a novel cancer therapy. Mol Cancer Ther. 2011;17(12):1636–40.

- 74. The Genome Sequence Archive Family. Toward Explosive Data Growth and Diverse Data Types. Genomics Proteomics Bioinformatics. 2021;19(4):578–83.
- 75. Database Resources of the National Genomics Data Center. China National Center for Bioinformation in 2022. Nucleic Acids Res. 2022;50(D1):D27–38.

Publisher's Note

Springer Nature remains neutral with regard to jurisdictional claims in published maps and institutional affiliations.